

# Inclusion of Methyl 2-Naphthalenecarboxylate and Dimethyl 2,3-, 2,6-, and 2,7-Naphthalenedicarboxylates by Cyclodextrins in Aqueous Solution

Sanyo Hamai

Department of Chemistry, Faculty of Education and Human Studies, Akita University,  
1-1 Tegata Gakuen-machi, Akita 010-8502

Received August 3, 2010; E-mail: hamai@ipc.akita-u.ac.jp

In aqueous solution, inclusion complexes of several naphthalenecarboxylate derivatives with  $\alpha$ -,  $\beta$ -,  $\gamma$ -, and heptakis(2,3,6-tri-*O*-methyl)- $\beta$ -cyclodextrin ( $\alpha$ -CD,  $\beta$ -CD,  $\gamma$ -CD, and TM- $\beta$ -CD) have been investigated by means of absorption and fluorescence spectroscopy.  $\beta$ -CD and TM- $\beta$ -CD form 1:1 inclusion complexes with methyl 2-naphthalenecarboxylate (2NC), dimethyl 2,7-naphthalenedicarboxylate (27DNC), dimethyl 2,6-naphthalenedicarboxylate (26DNC), and dimethyl 2,3-naphthalenedicarboxylate (23DNC).  $\alpha$ -CD forms a 2:1  $\alpha$ -CD–2NC inclusion complex as well as a 1:1 inclusion complex with 2NC. With 27DNC,  $\alpha$ -CD forms a 1:1 inclusion complex alone, whereas  $\alpha$ -CD forms a 2:1  $\alpha$ -CD–guest inclusion complex with 26DNC.  $\gamma$ -CD forms 1:1 inclusion complexes with all the naphthalenecarboxylate derivatives examined. In addition to the 1:1 inclusion complex,  $\gamma$ -CD forms a 2:2  $\gamma$ -CD–guest inclusion complex with 27DNC (or 26DNC) through the association of the 1:1 inclusion complexes. From the 2:2 inclusion complex, the excimer fluorescence of the guest has been observed. In the case of 23DNC,  $\gamma$ -CD forms a 1:2  $\gamma$ -CD–guest inclusion complex, from which no excimer fluorescence has been observed.

Commercially available cyclodextrins (CDs) are cyclic oligosaccharides consisting of six, seven, and eight D-glucopyranose residues, which are called  $\alpha$ -CD,  $\beta$ -CD, and  $\gamma$ -CD, respectively.<sup>1,2</sup> Due to a relatively hydrophobic cavity, CD accommodates an organic molecule of appropriate dimensions to form an inclusion complex. In most cases, a CD molecule accommodates a single guest molecule to form a 1:1 inclusion complex.<sup>3</sup> In some cases however, the CD cavity includes the same or different kind of guest molecule to form a 1:2 CD–guest or 1:1:1 CD–guest 1–guest 2 inclusion complex.<sup>4–10</sup> On the other hand, a long molecule can be incorporated into two CD cavities, forming a 2:1 CD–guest inclusion complex.<sup>11–13</sup>

A naphthalene ring snugly fits the  $\beta$ -CD cavity. It is too bulky for a single  $\alpha$ -CD molecule to thoroughly encapsulate a naphthalene ring. Because  $\alpha$ -CD is shallowly bound to a naphthalene derivative to form a 1:1 inclusion complex, part of a naphthalene derivative is extruded into the environment. Consequently, an additional  $\alpha$ -CD molecule may be bound to the extruded part of the naphthalene derivative to form a 2:1  $\alpha$ -CD–guest inclusion complex. The formation of 1:1 and 2:1  $\alpha$ -CD–guest inclusion complexes has been reported for 2-naphthol, 6-bromo-2-naphthol, naphthalene, 2-acetylnaphthalene, 2-chloronaphthalene, and 2-methylnaphthalene.<sup>14–19</sup> For  $\beta$ -CD, 2:1 host–guest inclusion complexes have been suggested for acenaphthene, *p*-nitro(trifluoroacetanilide), and propantheline bromide.<sup>20–22</sup>  $\gamma$ -CD, which has a cavity wider than those of  $\alpha$ - and  $\beta$ -CD, forms 1:2  $\gamma$ -CD–guest inclusion complexes with Methyl Orange, Methylene Blue, Pyronine Y, Toluidine Blue, thionine, and Thioflavin T.<sup>4,5,7,8,23,24</sup> For a long but slightly bent molecule such as 2,4-diphenyloxazole

(24DPO),  $\gamma$ -CD forms a 2:1  $\gamma$ -CD–guest inclusion.<sup>25</sup> On the other hand,  $\beta$ -CD, whose cavity is narrower than the  $\gamma$ -CD cavity, forms not a 2:1 but a 1:1  $\beta$ -CD–24DPO inclusion complex. Consequently, inclusion modes of CD depend on the shape of the guest molecule as well as CD.

For several naphthalene derivatives, it has been reported that  $\beta$ -CD or  $\gamma$ -CD forms 2:2 inclusion complexes, which are produced by the association of 1:1 CD–guest inclusion complexes.<sup>26–28</sup> The 2:2 inclusion complexes may emit excimer fluorescence, because two guest molecules of the same kind are located in the neighborhood within the CD cavities.

Inclusion complexes of  $\alpha$ -,  $\beta$ -, and  $\gamma$ -CD with methyl 2-naphthalenecarboxylate (2NC) and dimethyl 2,3-naphthalenedicarboxylate (23ND) have been investigated by means of fluorescence spectroscopy alone.<sup>29–32</sup> Mendicuti et al. also examined the formation of the inclusion complexes of  $\alpha$ - and  $\beta$ -CD with dimethyl 2,6-naphthalenedicarboxylate (26ND).<sup>33</sup> They have suggested that the stoichiometry of these inclusion complexes is 1:1 except for a 2:1  $\alpha$ -CD–26ND inclusion complex.<sup>33</sup> 2-Hydroxypropyl- $\alpha$ -,  $\beta$ -, and  $\gamma$ -cyclodextrins form 1:1 inclusion complexes with 2NC.<sup>34</sup>

In a series of spectroscopic studies on the formation of CD inclusion complexes, we have revealed that  $\alpha$ -CD forms 1:1 and 2:1 host–guest inclusion complexes with 2-substituted naphthalene such as 2-methylnaphthalene.<sup>15,18,19</sup> From this point of view, it may be expected that  $\alpha$ -CD forms a 2:1 inclusion complex with methyl 2-naphthalenecarboxylate, although only a 1:1  $\alpha$ -CD–2NC inclusion complex has been suggested.<sup>29</sup> Dimethyl 2,7-naphthalenedicarboxylate (27ND), whose inclusion complexes of CD have not been examined, is long but slightly bent, although 23ND and 26ND are long

but not bent molecules. The inclusion mode of CDs may be affected by the slightly different molecular shapes of the naphthalenedicarboxylates. Under some experimental conditions, there may be a possibility that the association occurs between 1:1 inclusion complexes of the monocarboxylate or dicarboxylate of naphthalene, although a relatively bulky methoxycarbonyl group(s) is substituted on a naphthalene ring. Thus, we tried to examine the inclusion modes of  $\alpha$ -,  $\beta$ -, and  $\gamma$ -CD for 2NC, 23ND, 26ND, and 27ND by means of absorption spectroscopy as well as fluorescence spectroscopy. In addition to  $\alpha$ -,  $\beta$ -, and  $\gamma$ -CD, inclusion complexation with heptakis(2,3,6-tri-*O*-methyl)- $\beta$ -cyclodextrin has been examined.

### Experimental

$\alpha$ -Cyclodextrin ( $\alpha$ -CD) and heptakis(2,3,6-tri-*O*-methyl)- $\beta$ -cyclodextrin (TM- $\beta$ -CD), which were purchased from Nacalai Tesque, Inc., were used as received.  $\beta$ -Cyclodextrin ( $\beta$ -CD) obtained from Nacalai Tesque, Inc. was twice recrystallized from water.  $\gamma$ -Cyclodextrin ( $\gamma$ -CD), which was purchased from Tokyo Chemical Industry Co., Ltd. was used as received. Methyl 2-naphthalenecarboxylate (2NC) obtained from Wako Pure Chemical Industries, Ltd. was recrystallized from a benzene–cyclohexane mixture. Dimethyl 2,3- and 2,7-naphthalenedicarboxylates (23DNC and 27DNC), which were obtained from Tokyo Chemical Industry Co., Ltd. and Wako Pure Chemical Industries, Ltd., respectively, were recrystallized from benzene. Dimethyl 2,6-naphthalenedicarboxylate (26DNC) obtained from Tokyo Chemical Industries, Ltd. was used as received.

The concentrations of 2NC, 23DNC, 26DNC, and 27DNC in aqueous solution were estimated under the assumptions that their molar absorption coefficients in water are the same as those in methanol, respectively.

Absorption spectra were recorded on a Shimadzu UV-2450 spectrophotometer. Fluorescence spectra were taken with a Shimadzu RF-501 spectrofluorometer equipped with a cooled Hamamatsu R-943 photomultiplier. The fluorescence spectra were corrected for the spectral response of the fluorometer. Spectroscopic measurements were made at  $25 \pm 0.1$  °C.

### Results and Discussion

**Inclusion Modes of 2NC. Absorption and Fluorescence Spectra of 2NC in the Presence of  $\beta$ -CD:** Figure 1a shows absorption spectra of 2NC ( $1.1 \times 10^{-5}$  mol dm $^{-3}$ ) in aqueous solution containing various concentrations of  $\beta$ -CD. Upon the addition of  $\beta$ -CD to 2NC solution, the absorption peaks of 2NC are shifted to longer wavelengths, suggesting the formation of an inclusion complex between  $\beta$ -CD and 2NC. Figure 2a exhibits fluorescence spectra of 2NC ( $2.2 \times 10^{-6}$  mol dm $^{-3}$ ) in aqueous solution containing various concentrations of  $\beta$ -CD. When  $\beta$ -CD is added, a fluorescence-band shoulder at about 370 nm is enhanced, and shifts to 368 nm, accompanied by a reduction in the intensity of the original peak at 389 nm. This fluorescence spectral change indicates the formation of an inclusion complex of  $\beta$ -CD with 2NC. Because a naphthalene ring snugly fits the  $\beta$ -CD cavity, it is expected that a 1:1 inclusion complex is formed between  $\beta$ -CD and 2NC.

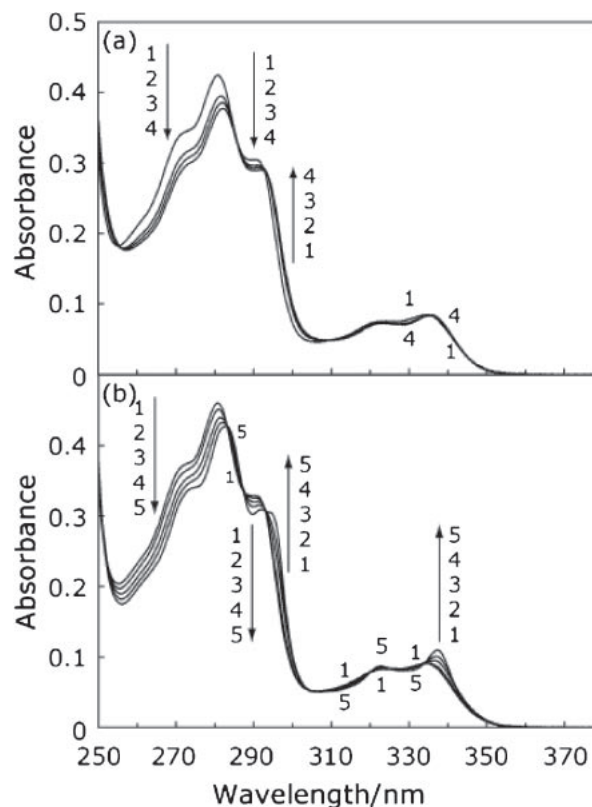


**Figure 1.** (a) Absorption spectra of 2NC ( $1.1 \times 10^{-5}$  mol dm $^{-3}$ ) in aqueous solution containing various concentrations of  $\beta$ -CD. Concentration of  $\beta$ -CD: (1) 0, (2)  $1.0 \times 10^{-3}$ , (3)  $3.0 \times 10^{-3}$ , and (4)  $1.0 \times 10^{-2}$  mol dm $^{-3}$ . (b) Absorption spectra of 2NC ( $1.2 \times 10^{-5}$  mol dm $^{-3}$ ) in aqueous solution containing various concentrations of  $\alpha$ -CD. Concentration of  $\alpha$ -CD: (1) 0, (2)  $1.0 \times 10^{-3}$ , (3)  $3.0 \times 10^{-3}$ , (4)  $5.0 \times 10^{-3}$ , and (5)  $1.0 \times 10^{-2}$  mol dm $^{-3}$ .



Here,  $K_1$  is the equilibrium constant for the formation of the 1:1  $\beta$ -CD–2NC inclusion complex ( $\beta$ -CD $\cdot$ 2NC). In this case, a double-reciprocal plot for the fluorescence intensity should be linear:

$$1/(I_f - I_f^0) = 1/a + 1/(aK_1[\gamma\text{-CD}]) \quad (2)$$

where  $I_f$  and  $I_f^0$  are the fluorescence intensity of 2NC in the presence and absence of  $\beta$ -CD, respectively, and  $a$  is an experimental constant including the fluorescence quantum yields of free 2NC and the 1:1  $\beta$ -CD–2NC inclusion complex. Figure 3 depicts a double-reciprocal plot for the fluorescence intensity of 2NC in the presence of  $\beta$ -CD. This plot shows a straight line, indicating that the 1:1 inclusion complex is formed between  $\beta$ -CD and 2NC. From the plot, the  $K_1$  value for  $\beta$ -CD is evaluated to be  $1700 \pm 100$  mol $^{-1}$  dm $^3$  (Table 1), which is slightly less than that ( $1965 \pm 159$  mol $^{-1}$  dm $^3$ ) reported by Mendicuti et al.<sup>29</sup>

**Inclusion Complexation of 2NC with  $\alpha$ -CD:** Figure 1b shows absorption spectra of 2NC ( $1.2 \times 10^{-5}$  mol dm $^{-3}$ ) in aqueous solution containing various concentrations of  $\alpha$ -CD. As the  $\alpha$ -CD concentration is increased, absorption peaks are

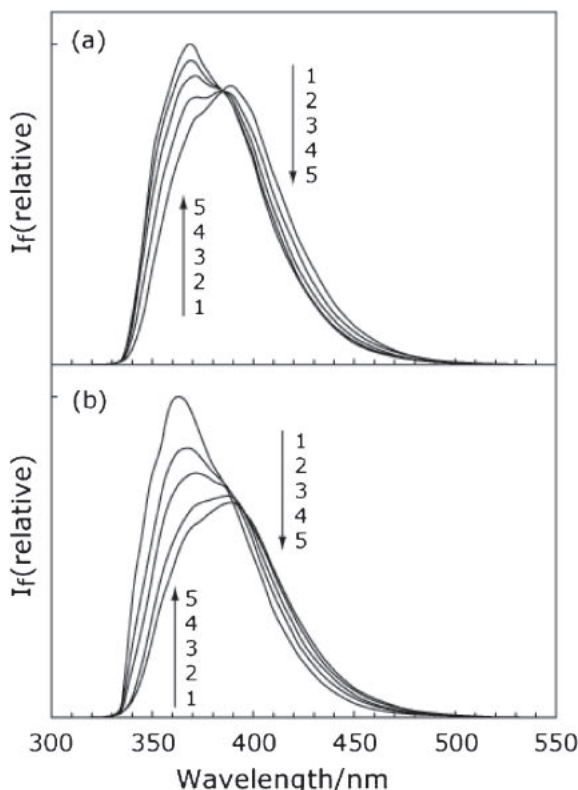


**Figure 2.** (a) Fluorescence spectra of 2NC ( $2.2 \times 10^{-6}$  mol dm $^{-3}$ ) in aqueous solution containing various concentrations of  $\beta$ -CD. Concentration of  $\beta$ -CD: (1) 0, (2)  $3.0 \times 10^{-4}$ , (3)  $1.0 \times 10^{-3}$ , (4)  $3.0 \times 10^{-3}$ , and (5)  $1.0 \times 10^{-2}$  mol dm $^{-3}$ .  $\lambda_{\text{ex}} = 295$  nm. (b) Fluorescence spectra of 2NC ( $2.2 \times 10^{-6}$  mol dm $^{-3}$ ) in aqueous solution containing various concentrations of  $\alpha$ -CD. Concentration of  $\alpha$ -CD: (1) 0, (2)  $1.0 \times 10^{-3}$ , (3)  $3.0 \times 10^{-3}$ , (4)  $5.0 \times 10^{-3}$ , and (5)  $1.0 \times 10^{-2}$  mol dm $^{-3}$ .  $\lambda_{\text{ex}} = 295$  nm.

shifted to longer wavelengths, suggesting the formation of an inclusion complex of  $\alpha$ -CD with 2NC. It should be noted that the absorption peaks are remarkably sharpened in the presence of  $\alpha$ -CD, compared to  $\beta$ -CD. The sharpening and shift of the peaks suggest that 2NC in  $\alpha$ -CD solution exists in a more hydrophobic environment. The  $\alpha$ -CD cavity, which is narrower than the  $\beta$ -CD cavity, cannot encapsulate a naphthalene ring deeply. Consequently, it is unreasonable that the absorption spectral change shown in Figure 1b is due only to the formation of the 1:1  $\alpha$ -CD–2NC inclusion complex. Such dramatic absorption spectral changes of naphthalene derivatives, which are in contrast to that in the presence of  $\beta$ -CD, are reported for 2-naphthol, 6-bromo-2-naphthol, naphthalene, 2-chloronaphthalene, and 2-methylnaphthalene.<sup>14,15,17–19</sup> The remarkable absorption spectral changes of naphthalene derivatives are due most likely to the formation of a 1:1  $\alpha$ -CD–naphthalene derivative inclusion complex followed by the formation of a 2:1  $\alpha$ -CD–naphthalene derivative. Within the two  $\alpha$ -CD cavities, the environment of a naphthalene derivative is more hydrophobic than that bound to a single  $\beta$ -CD cavity. This leads to the sharp absorption bands in the presence of  $\alpha$ -CD compared to  $\beta$ -CD.

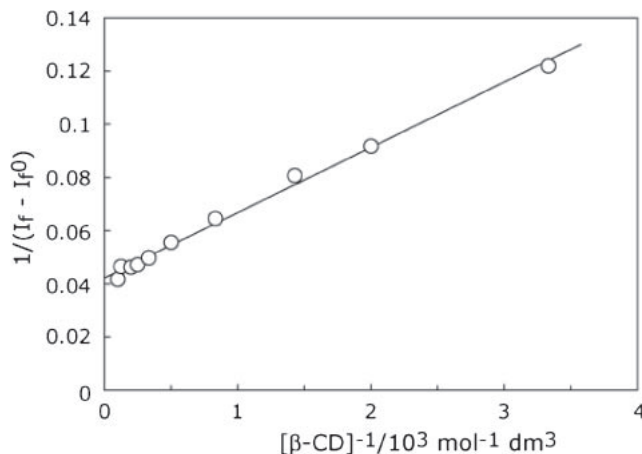


**Figure 3.** Double-reciprocal plot for 2NC ( $2.2 \times 10^{-6}$  mol dm $^{-3}$ ) in aqueous solution containing  $\beta$ -CD.  $\lambda_{\text{ex}} = 295$  nm.  $\lambda_{\text{obs}} = 370$  nm.

**Table 1.** The  $K_1$  Values of  $\beta$ -CD and TM- $\beta$ -CD for 2NC, 27DNC, 26DNC, and 23DNC

Host	Guest	$K_1/\text{mol}^{-1} \text{ dm}^3$
$\beta$ -CD	2NC	$1700 \pm 100$
	27DNC	$2460 \pm 80$
	26DNC	$1670 \pm 40$
	23DNC	$1680 \pm 40$
TM- $\beta$ -CD	2NC	$370 \pm 20$
	27DNC	$330 \pm 20$
	26DNC	$340 \pm 10$
	23DNC	$160 \pm 10$

Figure 2b exhibits fluorescence spectra of 2NC ( $2.4 \times 10^{-6}$  mol dm $^{-3}$ ) in aqueous solution containing various concentrations of  $\alpha$ -CD. Upon the addition of  $\alpha$ -CD, the fluorescence peak is shifted to shorter wavelengths, accompanied by an enhancement of the fluorescence intensity. In addition, significant fluorescence spectral change is observed by the addition of  $\alpha$ -CD, compared to  $\beta$ -CD. At an  $\alpha$ -CD concentration of  $1.0 \times 10^{-2}$  mol dm $^{-3}$ , the fluorescence peak is blue-shifted from 388 to 363 nm; a fluorescence peak shift of 25 nm in  $\alpha$ -CD solution is greater than that of 20 nm in  $\beta$ -CD solution. These findings suggest that a 2NC molecule within the  $\alpha$ -CD inclusion complex is located in a more hydrophobic environment than that within the  $\beta$ -CD inclusion complex. Therefore, the fluorescence spectral change as well as the absorption spectral change in the presence of  $\alpha$ -CD indicates the formation of the 2:1  $\alpha$ -CD–2NC inclusion complex ( $(\alpha\text{-CD})_2 \cdot 2\text{NC}$ ).



where  $K_2$  is the equilibrium constant for the formation of the 2:1  $\alpha$ -CD–2NC inclusion complex. Because the 2NC concentration is very low (the absorbance of 2NC solution is very small), the fluorescence intensity of a relevant species is proportional to its concentration. When the 2:1  $\alpha$ -CD–2NC inclusion complex is formed, the fluorescence intensity,  $I_f$ , of 2NC solution containing  $\alpha$ -CD is expressed as

**Table 2.** Equilibrium Constants of  $\alpha$ -CD and  $\gamma$ -CD for 2NC, 27DNC, 26DNC, and 23DNC

Host	Guest	$K_1/\text{mol}^{-1} \text{ dm}^3$	$K_2/\text{mol}^{-1} \text{ dm}^3$	$K_2'/\text{mol}^{-2} \text{ dm}^6$	$K_3/\text{mol}^{-1} \text{ dm}^3$	$K_3'/\text{mol}^{-1} \text{ dm}^3$
$\alpha$ -CD	2NC	243 <sup>a)</sup>	254 <sup>a)</sup>			
		317 <sup>b)</sup>	446 <sup>b)</sup>			
		375 <sup>c)</sup>	381 <sup>c)</sup>			
	27DNC	300 $\pm$ 50				
	26DNC			(9.6 $\pm$ 0.3) $\times 10^5$		
$\gamma$ -CD	23DNC <sup>d)</sup>					
	2NC	560 $\pm$ 20				
	27DNC	600 $\pm$ 50			2.71 $\times 10^6$	
	26DNC	310 $\pm$ 60			6.71 $\times 10^5$	
	23DNC	430 $\pm$ 60				3190 <sup>e)</sup>
						2970 <sup>f)</sup>
						2580 <sup>g)</sup>
						3180 <sup>h)</sup>

a) From absorbance data. b)  $\lambda_{\text{ex}} = 337.4 \text{ nm}$ ,  $\lambda_{\text{obs}} = 375 \text{ nm}$ . c)  $\lambda_{\text{ex}} = 295 \text{ nm}$ ,  $\lambda_{\text{obs}} = 375 \text{ nm}$ . d) An equilibrium constant could not be estimated. e)  $\lambda_{\text{ex}} = 309 \text{ nm}$ ,  $\lambda_{\text{obs}} = 375 \text{ nm}$ ,  $[23\text{DNC}]_0 = 9.7 \times 10^{-5} \text{ mol dm}^{-3}$ . f)  $\lambda_{\text{ex}} = 309 \text{ nm}$ ,  $\lambda_{\text{obs}} = 375 \text{ nm}$ ,  $[23\text{DNC}]_0 = 4.1 \times 10^{-5} \text{ mol dm}^{-3}$ . g)  $\lambda_{\text{ex}} = 309 \text{ nm}$ ,  $\lambda_{\text{obs}} = 390 \text{ nm}$ ,  $[23\text{DNC}]_0 = 9.7 \times 10^{-5} \text{ mol dm}^{-3}$ . h)  $\lambda_{\text{ex}} = 320 \text{ nm}$ ,  $\lambda_{\text{obs}} = 390 \text{ nm}$ ,  $[23\text{DNC}]_0 = 9.7 \times 10^{-5} \text{ mol dm}^{-3}$ .

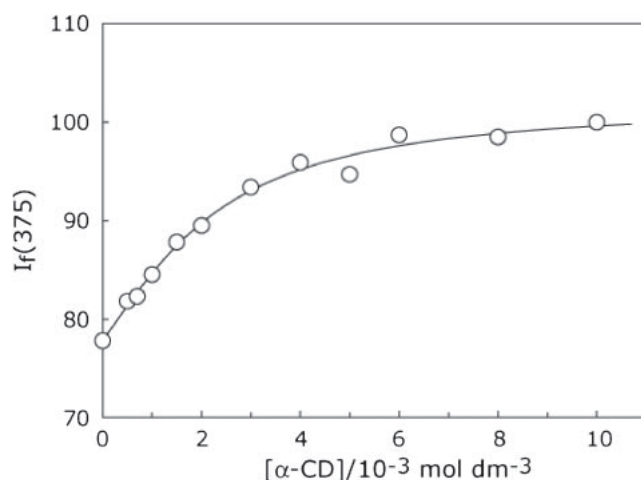


**Figure 4.** Simulation for the observed fluorescence intensities (open circles) of 2NC ( $2.2 \times 10^{-6} \text{ mol dm}^{-3}$ ) in aqueous solutions containing various concentrations of  $\alpha$ -CD. A best fit simulation curve, which has been based on the scheme involving the 1:1 and 2:1  $\alpha$ -CD–2NC inclusion complexes, has been calculated with assumed values of  $K_1$  ( $375 \text{ mol}^{-1} \text{ dm}^3$ ),  $K_2$  ( $381 \text{ mol}^{-1} \text{ dm}^3$ ),  $b$  ( $77.8 \text{ mol}^{-1} \text{ dm}^3$ ),  $c$  ( $96.4 \text{ mol}^{-1} \text{ dm}^3$ ), and  $d$  ( $102 \text{ mol}^{-1} \text{ dm}^3$ ).  $\lambda_{\text{ex}} = 295 \text{ nm}$ .  $\lambda_{\text{obs}} = 375 \text{ nm}$ .

$$\begin{aligned}
 I_f &= b[2\text{NC}] + c[\alpha\text{-CD} \cdot 2\text{NC}] + d[(\alpha\text{-CD})_2 \cdot 2\text{NC}] \\
 &= (b + cK_1[\alpha\text{-CD}] + dK_1K_2[\alpha\text{-CD}]^2)[2\text{NC}]_0 \\
 &\quad / (1 + K_1[\alpha\text{-CD}] + K_1K_2[\alpha\text{-CD}]^2) \quad (4)
 \end{aligned}$$

where  $b$ ,  $c$ , and  $d$  are experimental constants including the fluorescence quantum yields of free 2NC, the 1:1 inclusion complex, and the 2:1 inclusion complex, respectively.  $[2\text{NC}]_0$  is the initial concentration of 2NC.

Figure 4 illustrates the fluorescence intensity observed at 375 nm, which has been excited at 295 nm, as a function of the  $\alpha$ -CD concentration, and a best fit simulation curve, which has been calculated assuming values of  $b$ ,  $c$ ,  $d$ ,  $K_1$ , and  $K_2$

to be 77.8, 96.4, 102, 375, and 381  $\text{mol}^{-1} \text{ dm}^3$ , respectively (Table 2). We further simulated the fluorescence intensities excited at 337.4 nm, which is a peak wavelength of the  $^1\text{L}_a$  band of 2NC in the presence of  $\alpha$ -CD. From the simulation, the  $K_1$  and  $K_2$  values were evaluated to be 317 and 446  $\text{mol}^{-1} \text{ dm}^3$ , respectively. The  $K_1$  and  $K_2$  values obtained at an excitation wavelength of 337.4 nm were similar to those of 295 nm, respectively, supporting the existence of the 2:1  $\alpha$ -CD–2NC inclusion complex. To further confirm the formation of the 2:1 inclusion complex, we simulated the absorbance at 337.4 nm as a function of the  $\alpha$ -CD concentration. From the simulation, the  $K_1$  and  $K_2$  values were estimated to be 243 and 254  $\text{mol}^{-1} \text{ dm}^3$ , respectively, which have been similar to those obtained from the simulations using the fluorescence intensity. The result that the different methods gave similar  $K_1$  and  $K_2$  values, respectively, confirms the existence of the 2:1  $\alpha$ -CD–2NC inclusion complex.

A  $K_1$  value of  $202 \pm 17 \text{ mol}^{-1} \text{ dm}^3$  has been reported for the formation of the 1:1  $\alpha$ -CD–2NC inclusion complex, although the existence of the 2:1  $\alpha$ -CD–2NC inclusion complex has not been suggested.<sup>29</sup> Thus, under the assumption of the formation of only the 1:1  $\alpha$ -CD–2NC inclusion complex, we estimated the  $K_1$  value to be  $200 \pm 20 \text{ mol}^{-1} \text{ dm}^3$  from a double-reciprocal plot for the fluorescence intensity, of which measurement was made at an excitation and observation wavelength of 295 and 375 nm, respectively. However, a  $K_1$  value of  $27 \pm 11 \text{ mol}^{-1} \text{ dm}^3$  was evaluated from the double-reciprocal plot for the absorbance at 337.4 nm. Under the assumption of the formation of only the 1:1 inclusion complex, the  $K_1$  value obtained from the fluorescence intensity is not in agreement with that obtained from the absorbance data. The disagreement further confirms the formation of the 2:1  $\alpha$ -CD–2NC inclusion complex.

#### Inclusion Complexes of 2NC with $\gamma$ -CD and TM- $\beta$ -CD:

Absorption spectral change of 2NC by the addition of  $\gamma$ -CD or TM- $\beta$ -CD was similar to that by the addition of  $\beta$ -CD. This suggests the formation of an inclusion complex of 2NC with  $\gamma$ -CD or TM- $\beta$ -CD. When  $\gamma$ -CD was added, the fluorescence of



2NC was reduced in intensity. Upon the addition of TM- $\beta$ -CD, the fluorescence spectral change was similar to that upon the addition of  $\beta$ -CD. The fluorescence spectral change in the presence of  $\gamma$ -CD or TM- $\beta$ -CD indicates the formation of an inclusion complex with 2NC. From double-reciprocal plots for the fluorescence intensity, the  $K_1$  values for  $\gamma$ -CD and TM- $\beta$ -CD were evaluated to be  $560 \pm 20$  and  $370 \pm 20 \text{ mol}^{-1} \text{ dm}^3$ , respectively. These  $K_1$  values are less than that for  $\beta$ -CD. Because the cavity of  $\gamma$ -CD is wider than that of  $\beta$ -CD, 2NC does not snugly fit the  $\gamma$ -CD cavity, resulting in the relatively small  $K_1$  value. The TM- $\beta$ -CD cavity is deeper than the  $\beta$ -CD cavity. The interactions of a naphthalene ring of 2NC with the inner wall of the TM- $\beta$ -CD cavity may be weak compared to  $\beta$ -CD, although 2NC interacts with methyl groups substituted on the end(s) of the cavity. This would lead to the rather small  $K_1$  value of TM- $\beta$ -CD.

**Inclusion Modes of 27DNC. Inclusion Complexes of 27DNC with  $\alpha$ -,  $\beta$ -, and TM- $\beta$ -CD:** When  $\alpha$ -CD is added to 27DNC ( $4.2 \times 10^{-6} \text{ mol dm}^{-3}$ ) solution, absorption bands of 27DNC at 250 and 340 nm are very slightly shifted to longer wavelengths (Figure S1a). At the same time, the 250-nm band is slightly reduced in intensity. These findings suggest the formation of an inclusion complex of  $\alpha$ -CD with 27DNC. In the presence of  $\alpha$ -CD, the fluorescence intensity of 27DNC ( $4.2 \times 10^{-6} \text{ mol dm}^{-3}$ ) is increased (Figure 5a), suggesting the formation of the inclusion complex between  $\alpha$ -CD and 27DNC. A double-reciprocal plot for the fluorescence intensity exhibited a straight line, indicating a 1:1 stoichiometry for the  $\alpha$ -CD–27DNC inclusion complex. From the plot, a  $K_1$  value of  $300 \pm 50 \text{ mol}^{-1} \text{ dm}^3$  was evaluated for  $\alpha$ -CD.

As the  $\beta$ -CD concentration is increased, the absorption bands of 27DNC ( $4.3 \times 10^{-6} \text{ mol dm}^{-3}$ ) at 250 and 340 nm decrease in intensity, suggesting the formation of an inclusion complex of  $\beta$ -CD with 27DNC (Figure S1b). Upon the addition of  $\beta$ -CD, the fluorescence peaks of 27DNC ( $4.3 \times 10^{-6} \text{ mol dm}^{-3}$ ) are intensified, accompanied by a slight peak shift to shorter wavelengths (Figure 5b), indicating the formation of an inclusion complex of  $\beta$ -CD with 27DNC. As in the case of  $\alpha$ -CD, a double-reciprocal plot for the fluorescence intensity exhibited a straight line, indicating the formation of the 1:1  $\beta$ -CD–27DNC inclusion complex. From the plot, the  $K_1$  value for  $\beta$ -CD was evaluated to be  $2460 \pm 80 \text{ mol}^{-1} \text{ dm}^3$ , which is about eight times greater than the  $K_1$  value ( $300 \pm 50 \text{ mol}^{-1} \text{ dm}^3$ ) for  $\alpha$ -CD. This implies that the  $\beta$ -CD cavity deeply encapsulates a 27DNC molecule, while the  $\alpha$ -CD shallowly encapsulates one.

In the case of TM- $\beta$ -CD, the absorption and fluorescence spectral changes of 27DNC were similar to those for  $\beta$ -CD, respectively, indicating the formation of an inclusion complex of TM- $\beta$ -CD with 27DNC. From the fluorescence intensity change, a  $K_1$  value of  $330 \pm 20 \text{ mol}^{-1} \text{ dm}^3$  was obtained for TM- $\beta$ -CD. This  $K_1$  value is about eight times less than that for  $\beta$ -CD. Because the cavity of TM- $\beta$ -CD is deeper than that of  $\beta$ -CD, a naphthalene ring with two methoxycarbonyl groups, which are substituted on a cis-like position with respect to the longitudinal axis of the naphthalene ring, may not be deeply incorporated into the TM- $\beta$ -CD cavity: the interactions of the naphthalene ring with the inner wall of the TM- $\beta$ -CD cavity may be weaker than those of the  $\beta$ -CD cavity. This leads to the

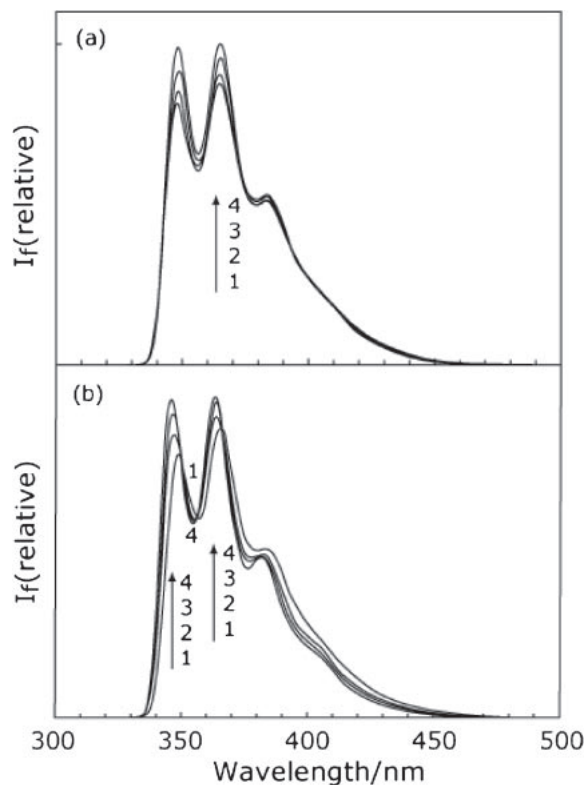


**Figure 5.** (a) Fluorescence spectra of 27DNC ( $4.2 \times 10^{-6} \text{ mol dm}^{-3}$ ) in aqueous solution containing various concentrations of  $\alpha$ -CD. Concentration of  $\alpha$ -CD: (1) 0, (2)  $1.0 \times 10^{-3}$ , (3)  $3.0 \times 10^{-3}$ , and (4)  $1.0 \times 10^{-2} \text{ mol dm}^{-3}$ .  $\lambda_{\text{ex}} = 290 \text{ nm}$ . (b) Fluorescence spectra of 27DNC ( $4.2 \times 10^{-6} \text{ mol dm}^{-3}$ ) in aqueous solution containing various concentrations of  $\beta$ -CD. Concentration of  $\beta$ -CD: (1) 0, (2)  $1.0 \times 10^{-3}$ , (3)  $3.0 \times 10^{-3}$ , and (4)  $1.0 \times 10^{-2} \text{ mol dm}^{-3}$ .  $\lambda_{\text{ex}} = 290 \text{ nm}$ .

small  $K_1$  value for TM- $\beta$ -CD. Similar trend that the  $K_1$  value for TM- $\beta$ -CD is significantly less than that for  $\beta$ -CD is observed for 2NC (Table 1).

**Inclusional Complexation of 27DNC with  $\gamma$ -CD:** Figure 6 depicts absorption spectra of 27DNC ( $4.2 \times 10^{-6} \text{ mol dm}^{-3}$ ) in aqueous solution containing various concentrations of  $\gamma$ -CD. With an increase in the  $\gamma$ -CD concentration, the absorption peaks are significantly reduced in intensity. In addition, the absorption peaks at 250 and 340 nm are shifted to shorter and longer wavelengths, respectively, suggesting the formation of an inclusion complex of  $\gamma$ -CD with 27DNC. Figures 7a and 7b show fluorescence spectra of concentrated ( $4.2 \times 10^{-6} \text{ mol dm}^{-3}$ ) and dilute ( $4.2 \times 10^{-7} \text{ mol dm}^{-3}$ ) 27DNC solution containing various concentrations of  $\gamma$ -CD, respectively. In the both solutions, the fluorescence intensity is remarkably reduced by the addition of  $\gamma$ -CD, compared to  $\alpha$ - and  $\beta$ -CD. For concentrated 27DNC solution, a new broad fluorescence band appears in the longer-wavelength region, whereas no new band at longer wavelengths appears for dilute 27DNC solution. Therefore, the new longer-wavelength band is due most likely to the excimer fluorescence of 27DNC, which arises from an inclusion complex between  $\gamma$ -CD and 27DNC.

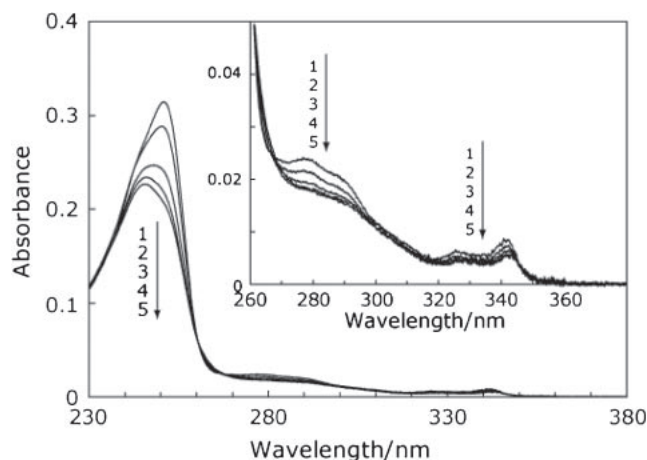
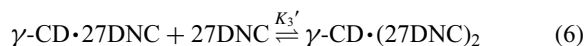


**Figure 6.** Absorption spectra of 27DNC ( $4.2 \times 10^{-6}$  mol dm $^{-3}$ ) in aqueous solution containing various concentrations of  $\gamma$ -CD. Concentration of  $\gamma$ -CD: (1) 0, (2)  $3.0 \times 10^{-4}$ , (3)  $1.0 \times 10^{-3}$ , (4)  $3.0 \times 10^{-3}$ , and (5)  $1.0 \times 10^{-2}$  mol dm $^{-3}$ .

In dilute solution of 27DNC, only a 1:1  $\gamma$ -CD–27DNC inclusion complex is most likely formed. In fact, a double-reciprocal plot for the fluorescence intensity exhibits a good straight line (Figure S2), indicating the formation of the 1:1  $\gamma$ -CD–27DNC inclusion complex. From the plot, a  $K_1$  value of  $600 \pm 50$  mol $^{-1}$  dm $^3$  is estimated. The excimer fluorescence at a high 27DNC concentration may be due to a 2:2  $\gamma$ -CD–27DNC inclusion complex ( $(\gamma\text{-CD})_2 \cdot (27\text{DNC})_2$ ), which is produced by the association of the 1:1  $\gamma$ -CD–27DNC inclusion complexes, or a 1:2  $\gamma$ -CD–27DNC inclusion complex ( $\gamma\text{-CD} \cdot (27\text{DNC})_2$ ), which is produced by the association of the 1:1  $\gamma$ -CD–27DNC inclusion complex with an additional 27DNC molecule.



or



Here,  $K_3$  and  $K_3'$  is the equilibrium constant for the formation of the 2:2  $\gamma$ -CD–27DNC inclusion complex and that of the 1:2  $\gamma$ -CD–27DNC inclusion complex, respectively.

When the 2:2  $\gamma$ -CD–27DNC inclusion complex is responsible for the excimer fluorescence, the intensity of the excimer fluorescence,  $I_f(\text{excimer})$ , is represented by

$$\begin{aligned} I_f(\text{excimer}) &= e[(\gamma\text{-CD})_2 \cdot (27\text{DNC})_2] \\ &= eK_1^2 K_3 [\gamma\text{-CD}]^2 [27\text{DNC}]^2 \end{aligned} \quad (7)$$

where  $e$  is an experimental constant including the quantum yield of the excimer fluorescence from the 2:2 inclusion complex. Using an assumed  $K_3$  value, the concentration of free 27DNC can be calculated from the quadratic equation concerning the concentration of free 27DNC.

$$\begin{aligned} 2K_1^2 K_3 [\gamma\text{-CD}]^2 [27\text{DNC}]^2 \\ + (1 + K_1 [\gamma\text{-CD}]) [27\text{DNC}] - [27\text{DNC}]_0 = 0 \end{aligned} \quad (8)$$

where  $[27\text{DNC}]_0$  is the initial concentration of 27DNC. Figure 8 exhibits the intensity of the excimer fluorescence at 450 nm, and a best fit simulation curve (solid curve). The best fit simulation curve has been calculated assuming the values of

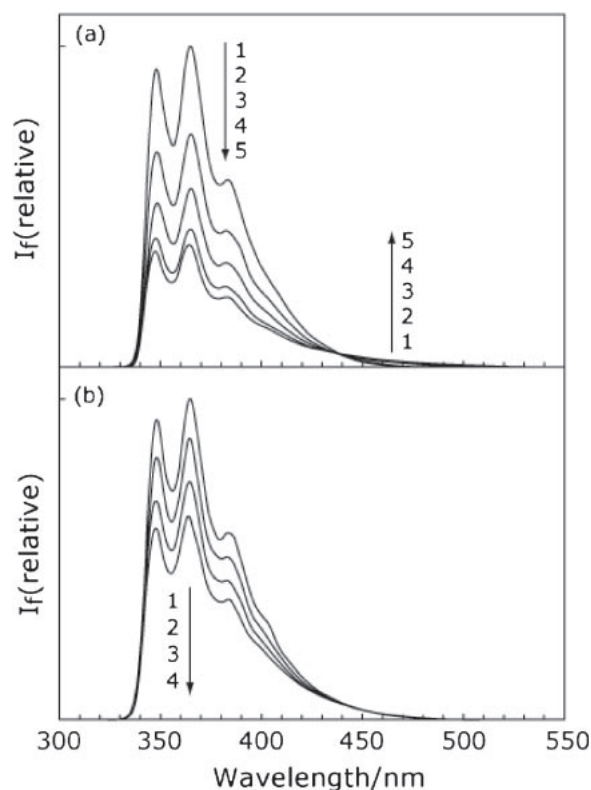


**Figure 7.** (a) Fluorescence spectra of concentrated 27DNC ( $4.2 \times 10^{-6}$  mol dm $^{-3}$ ) solution containing various concentrations of  $\gamma$ -CD. Concentration of  $\gamma$ -CD: (1) 0, (2)  $3.0 \times 10^{-4}$ , (3)  $1.0 \times 10^{-3}$ , (4)  $3.0 \times 10^{-3}$ , and (5)  $1.0 \times 10^{-2}$  mol dm $^{-3}$ .  $\lambda_{\text{ex}} = 290$  nm. (b) Fluorescence spectra of dilute 27DNC ( $4.2 \times 10^{-7}$  mol dm $^{-3}$ ) solution containing various concentrations of  $\gamma$ -CD. Concentration of  $\gamma$ -CD: (1) 0, (2)  $3.0 \times 10^{-4}$ , (3)  $1.0 \times 10^{-3}$ , and (4)  $3.0 \times 10^{-3}$  mol dm $^{-3}$ .  $\lambda_{\text{ex}} = 290$  nm.

$e$  and  $K_3$  to be  $2.93 \times 10^7$  and  $2.71 \times 10^6$  mol $^{-1}$  dm $^3$ , respectively, because the  $K_1$  value for  $\gamma$ -CD has been already evaluated. The best fit simulation curve well fit the observed excimer-fluorescence intensities, indicating that 2:2  $\gamma$ -CD–27DNC inclusion complex is responsible for the excimer fluorescence. The  $K_1^2 K_3$  value, which is the equilibrium constant for the formation of the 2:2 inclusion complex from  $\gamma$ -CD and free 27DNC, is calculated to be  $9.76 \times 10^{11}$  mol $^{-3}$  dm $^9$ . This value is slightly greater than the  $K_1^2 K_3$  values ( $1 \times 10^8$ – $6 \times 10^{11}$  mol $^{-3}$  dm $^9$ ) reported for 2-methylnaphthalene, 1-chloronaphthalene, etc.<sup>26b,35</sup>

If the 1:2  $\gamma$ -CD–27DNC inclusion complex is responsible for the excimer fluorescence, its intensity is represented as

$$\begin{aligned} I_f(\text{excimer}) &= f[\gamma\text{-CD} \cdot (27\text{DNC})_2] \\ &= fK_1 K_3' [\gamma\text{-CD}] [27\text{DNC}]^2 \end{aligned} \quad (9)$$

where  $f$  is an experimental constant including the quantum yield of the excimer fluorescence from the 1:2 inclusion complex. The concentration of free 27DNC can be calculated from the quadratic equation, assuming a  $K_3'$  value.

$$\begin{aligned} 2K_1 K_3' [\gamma\text{-CD}] [27\text{DNC}]^2 \\ + (1 + K_1 [\gamma\text{-CD}]) [27\text{DNC}] - [27\text{DNC}]_0 = 0 \end{aligned} \quad (10)$$

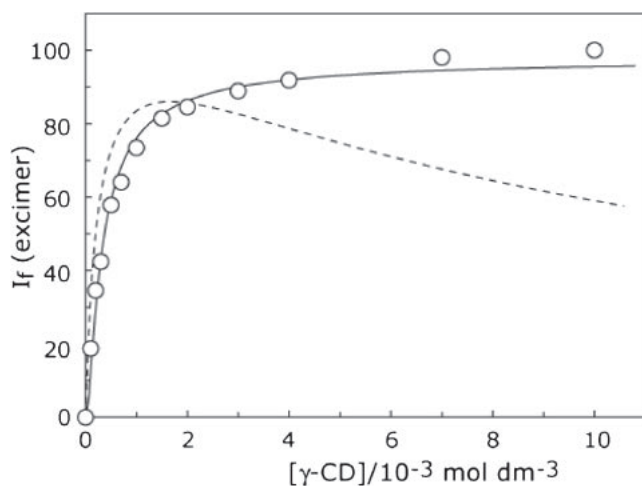


**Figure 8.** Simulation for the observed excimer fluorescence intensities (open circles) of 27DNC ( $7.8 \times 10^{-6} \text{ mol dm}^{-3}$ ) in aqueous solutions containing various concentrations of  $\gamma$ -CD. A best fit simulation curve (solid curve), which has been based on the scheme involving the 2:2  $\gamma$ -CD–27DNC inclusion complex, has been calculated with an evaluated  $K_1$  value of  $600 \text{ mol}^{-1} \text{ dm}^3$  and an assumed  $K_2$  value of  $2.71 \times 10^6 \text{ mol}^{-1} \text{ dm}^3$ . A best fit simulation curve (dotted curve), which has been based on the scheme involving the 1:2  $\gamma$ -CD–27DNC inclusion complex, has been calculated with an evaluated  $K_1$  value of  $600 \text{ mol}^{-1} \text{ dm}^3$  and an assumed  $K_2'$  value of  $2.38 \times 10^5 \text{ mol}^{-1} \text{ dm}^3$ .  $\lambda_{\text{ex}} = 290 \text{ nm}$ .  $\lambda_{\text{obs}} = 450 \text{ nm}$ .

In Figure 8, a best fit simulation curve based on the scheme, in which the 1:2  $\gamma$ -CD–27DNC inclusion complex is formed, is exhibited as a dashed curve. The simulation curve does not reproduce the observed fluorescence intensity data, indicating that the 1:2 inclusion complex is not responsible for the excimer fluorescence.

**Inclusion Modes of 26DNC. Inclusion Complexes of 26DNC with  $\alpha$ -,  $\beta$ -, and TM- $\beta$ -CD:** Figures 9a and 9b show absorption spectra of 26DNC in aqueous solution containing various concentrations of  $\alpha$ -CD and  $\beta$ -CD, respectively. These absorption spectral changes indicate the formation of inclusion complexes of  $\alpha$ - and  $\beta$ -CD with 26DNC. As in the case of 2NC, the absorption spectral change in the presence of  $\alpha$ -CD is more drastic than that in the presence of  $\beta$ -CD, suggesting that a 2:1  $\alpha$ -CD–26DNC inclusion complex is formed. Figures 10a and 10b exhibit fluorescence spectra of 26DNC in aqueous solution containing various concentrations of  $\alpha$ - and  $\beta$ -CD, respectively. As in the case of the absorption bands, the fluorescence bands in the presence of  $\alpha$ -CD are significantly sharpened compared to  $\beta$ -CD. This finding indicates the formation of the 2:1  $\alpha$ -CD–26DNC inclusion complex. Similar fluorescence spectral changes of 26DNC for  $\alpha$ - and  $\beta$ -CD have been reported by Mendicuti et al.<sup>33</sup> Figure 11a depicts a double-reciprocal plot for the fluorescence of 26DNC in  $\alpha$ -CD solution. This plot shows a concave curve, indicating that a stoichiometry of an  $\alpha$ -CD–26DNC inclusion complex is not 1:1. When the 2:1  $\alpha$ -CD–26DNC inclusion complex  $((\alpha\text{-CD})_2 \cdot 26\text{DNC})$  is formed, there is the equilibrium:

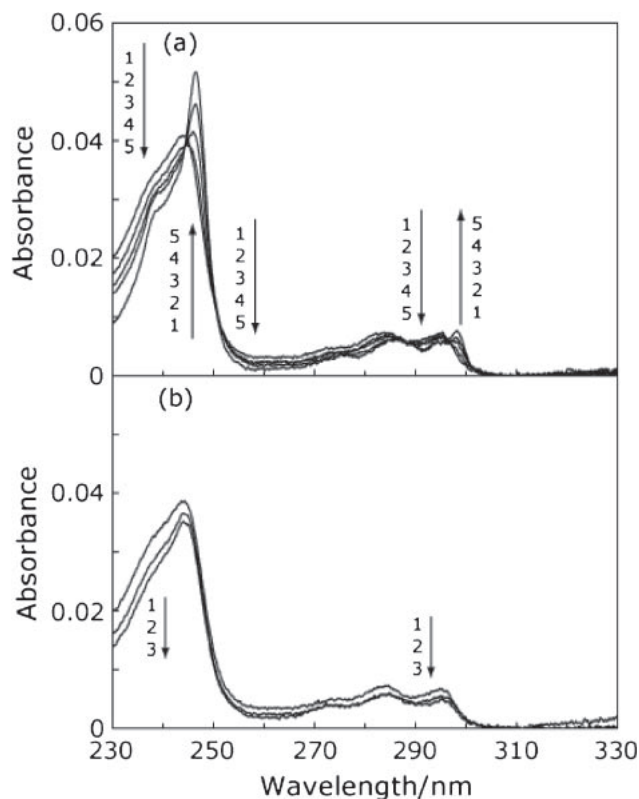
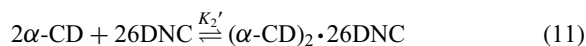


**Figure 9.** (a) Absorption spectra of 26DNC ( $4.6 \times 10^{-7} \text{ mol dm}^{-3}$ ) in aqueous solution containing various concentrations of  $\alpha$ -CD. Concentration of  $\alpha$ -CD: (1) 0, (2)  $5.0 \times 10^{-4}$ , (3)  $1.0 \times 10^{-3}$ , (4)  $2.0 \times 10^{-3}$ , and (5)  $1.0 \times 10^{-2} \text{ mol dm}^{-3}$ . (b) Absorption spectra of 26DNC ( $4.5 \times 10^{-7} \text{ mol dm}^{-3}$ ) in aqueous solution containing various concentrations of  $\beta$ -CD. Concentration of  $\beta$ -CD: (1) 0, (2)  $3.0 \times 10^{-3}$ , and (3)  $1.0 \times 10^{-2} \text{ mol dm}^{-3}$ .



In this case, the following equation holds for the fluorescence intensity of 26DNC in solution containing  $\alpha$ -CD.

$$1/(I_f - I_f^0) = 1/a' + 1/(a' K_2' [\alpha\text{-CD}]^2) \quad (12)$$

where  $a'$  is an experimental constant including the fluorescence quantum yields of free 26DNC and the 2:1  $\alpha$ -CD–26DNC inclusion complex. Figure 11b illustrates a plot of  $1/(I_f - I_f^0)$  against  $1/[\alpha\text{-CD}]^2$ . This plot exhibits a straight line, indicating the formation of the 2:1  $\alpha$ -CD–26DNC inclusion complex. From the plot, the  $K_2'$  value is evaluated to be  $(9.6 \pm 0.3) \times 10^5 \text{ mol}^{-2} \text{ dm}^6$ , which is slightly greater than the reported one  $((8.19 \pm 0.59) \times 10^5 \text{ mol}^{-2} \text{ dm}^6)$ .<sup>33</sup>

In the inclusion complex, in which two CD molecules are included, the secondary hydroxy-group ends of the two CD cavities associate with each other through hydrogen bonds.<sup>36</sup> Because the  $\alpha$ -CD cavity is narrow, two  $\alpha$ -CD molecules, whose cavities accommodate a slightly bent 27DNC molecule, may not associate with each other through hydrogen bonding. Consequently, a 2:1  $\alpha$ -CD–27DNC inclusion complex would not be formed. In the case of a linear 26DNC molecule, however, two  $\alpha$ -CD molecules, whose cavities accommodate a 26DNC molecule, most likely associate with each other to form the 2:1  $\alpha$ -CD–26DNC inclusion complex.

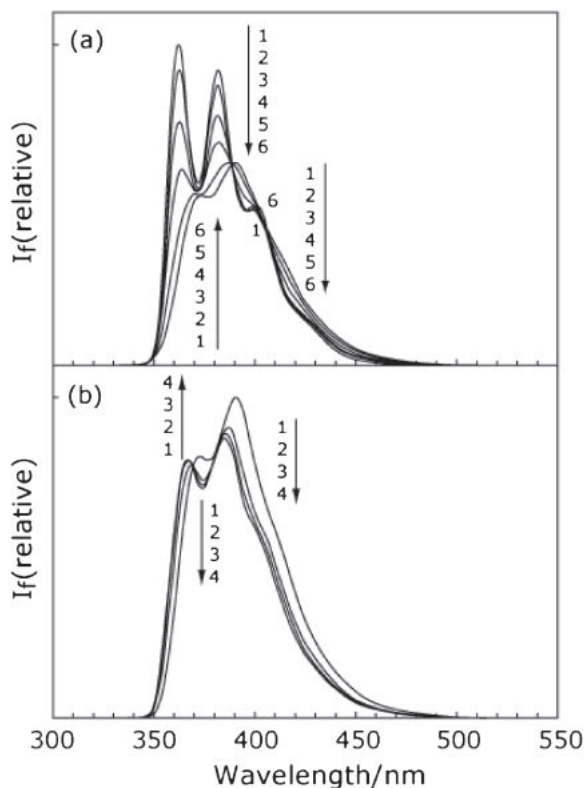


**Figure 10.** (a) Fluorescence spectra of 26DNC ( $4.6 \times 10^{-7}$  mol dm $^{-3}$ ) solution containing various concentrations of  $\alpha$ -CD. Concentration of  $\alpha$ -CD: (1) 0, (2)  $5.0 \times 10^{-4}$ , (3)  $1.0 \times 10^{-3}$ , (4)  $2.0 \times 10^{-3}$ , (5)  $4.0 \times 10^{-3}$ , and (6)  $1.0 \times 10^{-2}$  mol dm $^{-3}$ .  $\lambda_{\text{ex}} = 290$  nm. (b) Fluorescence spectra of 26DNC ( $4.5 \times 10^{-7}$  mol dm $^{-3}$ ) solution containing various concentrations of  $\beta$ -CD. Concentration of  $\beta$ -CD: (1) 0, (2)  $1.0 \times 10^{-3}$ , (3)  $3.0 \times 10^{-3}$ , and (4)  $1.0 \times 10^{-2}$  mol dm $^{-3}$ .  $\lambda_{\text{ex}} = 290$  nm.

For a 1:1  $\beta$ -CD–26DNC inclusion complex, a  $K_1$  value of  $1670 \pm 40$  mol $^{-1}$  dm $^3$ , which is less than the  $K_1$  value for 27DNC, has been obtained from the fluorescence intensity change. The  $K_1$  value for 26DNC is slightly greater than the reported one ( $1311 \pm 57$  mol $^{-1}$  dm $^3$ ).<sup>33</sup> The fluorescence spectral change of 26DNC in the presence of TM- $\beta$ -CD is similar to that in the presence of  $\beta$ -CD. The  $K_1$  value for TM- $\beta$ -CD has been estimated to be  $340 \pm 10$  mol $^{-1}$  dm $^3$ , which is nearly the same as that ( $330 \pm 20$  mol $^{-1}$  dm $^3$ ) of 27DNC.

**Interactions of 26DNC with  $\gamma$ -CD:** Figure 12 shows absorption and fluorescence spectra of 26DNC ( $3.2 \times 10^{-6}$  mol dm $^{-3}$ ) in aqueous solution containing various concentrations of  $\gamma$ -CD. The absorption spectral change for  $\gamma$ -CD, which suggests the formation of an inclusion complex of  $\gamma$ -CD with 26DNC, is similar to that for  $\beta$ -CD, although the significant spectral change is observed for  $\gamma$ -CD compared to  $\beta$ -CD. Upon the addition of a small amount of  $\gamma$ -CD (below about  $3 \times 10^{-3}$  mol dm $^{-3}$ ), the fluorescence intensity is reduced without a peak shift, accompanied by an enhancement of the fluorescence intensity in the longer wavelength region. At high concentrations of  $\gamma$ -CD, the fluorescence peaks are shifted to shorter wavelengths in spite of rather small decrease in the fluorescence intensity. The fluorescence spectral change reminds us

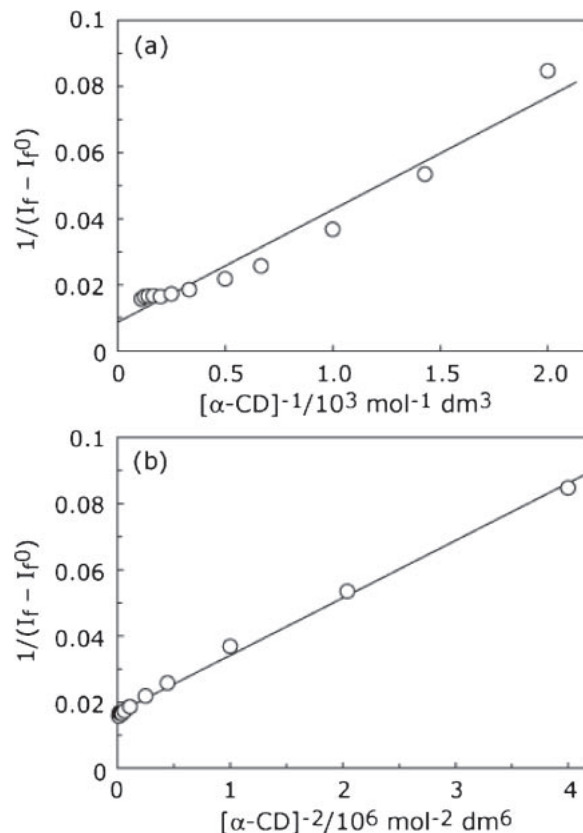


**Figure 11.** (a) Double-reciprocal plot for 26DNC ( $4.6 \times 10^{-7}$  mol dm $^{-3}$ ) in aqueous solution containing  $\alpha$ -CD.  $\lambda_{\text{ex}} = 290$  nm.  $\lambda_{\text{obs}} = 362$  nm. (b) Plot of  $1/(I_f - I_f^0)$  for 26DNC ( $4.6 \times 10^{-7}$  mol dm $^{-3}$ ) against  $1/[\alpha\text{-CD}]^2$ .  $\lambda_{\text{ex}} = 290$  nm.  $\lambda_{\text{obs}} = 362$  nm.

the existence of at least two kinds of inclusion complexes. When the 26DNC concentration was decreased to  $6.4 \times 10^{-7}$  mol dm $^{-3}$ , little or no fluorescence enhancement in the longer wavelength region was observed by the addition of  $\gamma$ -CD, suggesting that only a 1:1  $\gamma$ -CD–26DNC inclusion complex is formed in dilute 26DNC solution. Consequently, the fluorescence band at the longer wavelength tail is most likely assigned to the excimer fluorescence of 26DNC. From the fluorescence intensity change for dilute 26DNC solution, a  $K_1$  value of  $310 \pm 10$  mol $^{-1}$  dm $^3$  was obtained for  $\gamma$ -CD (Figure S3). This  $K_1$  value is about half of that for 27DNC.

As in the case of 27DNC, a 2:2  $\gamma$ -CD–26DNC inclusion complex may be responsible for the excimer fluorescence. Figure 13 illustrates the excimer fluorescence intensity observed at 460 nm as a function of the  $\gamma$ -CD concentration, and a best fit simulation curve (solid curve), which is based on the scheme involving the 2:2 inclusion complex, calculated assuming a  $K_3$  value of  $6.71 \times 10^5$  mol $^{-1}$  dm $^3$ . The best fit simulation curve well fits the observed excimer fluorescence intensities, indicating that the 2:2  $\gamma$ -CD–26DNC inclusion complex is responsible for the excimer fluorescence. To confirm the existence of the 2:2 inclusion complex, we have further calculated a best fit curve (dotted curve), which has been simulated according to the scheme involving the 1:2  $\gamma$ -CD–26DNC inclusion complex. However, the best fit simu-



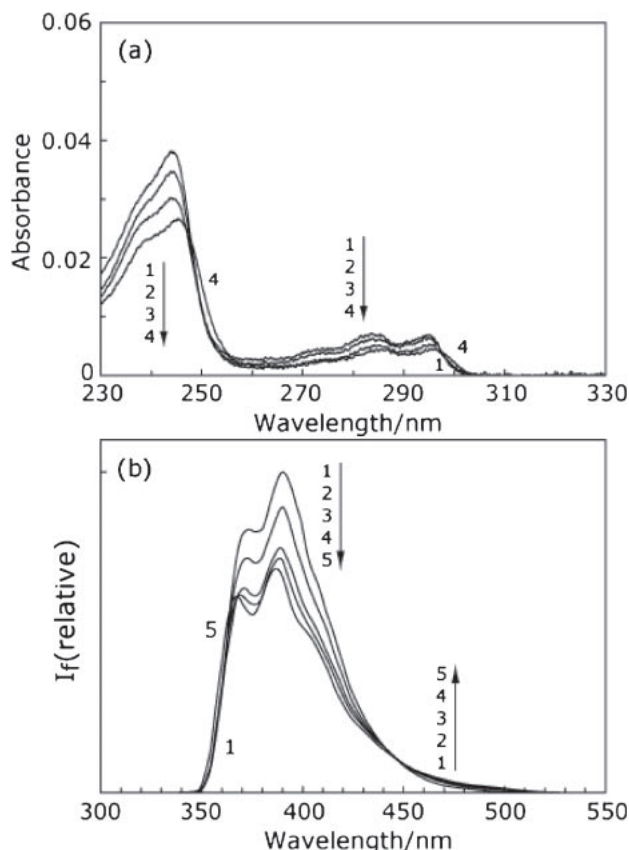


**Figure 12.** (a) Absorption spectra of 26DNC ( $4.4 \times 10^{-7}$  mol dm $^{-3}$ ) solution containing various concentrations of  $\gamma$ -CD. Concentration of  $\gamma$ -CD: (1) 0, (2)  $1.0 \times 10^{-3}$ , (3)  $3.0 \times 10^{-3}$ , and (4)  $1.0 \times 10^{-2}$  mol dm $^{-3}$ . (b) Fluorescence spectra of 26DNC ( $4.4 \times 10^{-7}$  mol dm $^{-3}$ ) solution containing various concentrations of  $\gamma$ -CD. Concentration of  $\gamma$ -CD: (1) 0, (2)  $1.0 \times 10^{-3}$ , (3)  $3.0 \times 10^{-3}$ , (4)  $5.0 \times 10^{-3}$ , and (5)  $1.0 \times 10^{-2}$  mol dm $^{-3}$ .  $\lambda_{\text{ex}} = 290$  nm.

lation curve based on the latter scheme does not reproduce the observed excimer fluorescence data, supporting that the excimer fluorescence is due to not the 1:2 but the 2:2 inclusion complex.

**Inclusion Modes of 23DNC. Inclusion Complexes of 23DNC with  $\beta$ -CD and TM- $\beta$ -CD:** Figure 14 displays absorption and fluorescence spectra of 23DNC ( $9.7 \times 10^{-5}$  and  $4.8 \times 10^{-5}$  mol dm $^{-3}$  for absorption and fluorescence spectra, respectively) in aqueous solution containing various concentrations of  $\beta$ -CD. When  $\beta$ -CD is added, the absorption peaks are decreased in intensity, suggesting the formation of an inclusion complex of  $\beta$ -CD with 23DNC. With an increase in the  $\beta$ -CD concentration, the fluorescence band is shifted to shorter wavelengths, indicating the formation of the inclusion complex between  $\beta$ -CD and 23DNC. From the fluorescence intensity change, the  $K_1$  value of 23DNC for  $\beta$ -CD has been evaluated to be  $1680 \pm 40$  mol $^{-1}$  dm $^3$ , which is nearly the same as those ( $1700 \pm 100$  and  $1670 \pm 40$  mol $^{-1}$  dm $^3$ ) of 2NC and 26DNC (Table 1). This result suggests that a naphthalene ring of 2NC, 23DNC, and 26DNC is thoroughly encapsulated in the  $\beta$ -CD cavity. The  $K_1$  value of 23DNC is greater than the reported one ( $1058.0 \pm 15.2$  mol $^{-1}$  dm $^3$ ).<sup>32</sup>

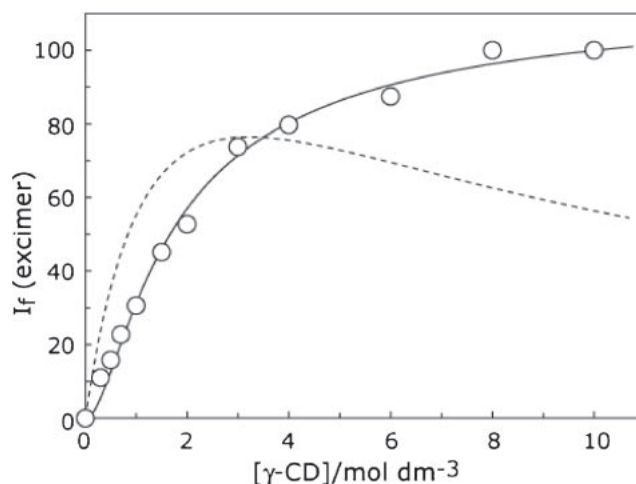


**Figure 13.** Simulation for the observed excimer fluorescence intensities (open circles) of 26DNC ( $4.4 \times 10^{-7}$  mol dm $^{-3}$ ) in aqueous solutions containing various concentrations of  $\gamma$ -CD. A best fit simulation curve (solid curve), based on the scheme involving the 2:2  $\gamma$ -CD–26DNC inclusion complex, has been calculated with an evaluated  $K_1$  value of  $310$  mol $^{-1}$  dm $^3$  of and an assumed  $K_2$  value of  $6.71 \times 10^5$  mol $^{-1}$  dm $^3$ . A best fit simulation curve (dotted curve), based on the scheme involving the 1:2  $\gamma$ -CD–26DNC inclusion complex, has been calculated with an evaluated  $K_1$  value of  $310$  mol $^{-1}$  dm $^3$  and an assumed  $K_2'$  value of  $2.23$  mol $^{-1}$  dm $^3$ .  $\lambda_{\text{ex}} = 290$  nm.  $\lambda_{\text{obs}} = 460$  nm.

For TM- $\beta$ -CD, the  $K_1$  value of 23DNC has been estimated to be  $160 \pm 10$  mol $^{-1}$  dm $^3$ , which is about half of those ( $370 \pm 20$ ,  $340 \pm 10$ , and  $330 \pm 20$  mol $^{-1}$  dm $^3$ ) of 2NC, 26DNC, and 27DNC (Table 1). We could not estimate the  $K_1$  value of 23DNC for  $\alpha$ -CD, because the fluorescence intensity change was very small in the  $\alpha$ -CD concentration range of up to  $1.0 \times 10^{-2}$  mol dm $^{-3}$ .

**Inclusion Complexes of 23DNC with  $\gamma$ -CD:** Absorption spectral change of 23DNC ( $9.7 \times 10^{-5}$  mol dm $^{-3}$ ) in aqueous solution containing  $\gamma$ -CD has been similar to that containing  $\beta$ -CD, suggesting the formation of an inclusion complex between  $\gamma$ -CD and 23DNC. Figures 15a and 15b exhibit fluorescence spectra of concentrated ( $9.7 \times 10^{-5}$  mol dm $^{-3}$ ) and dilute ( $1.1 \times 10^{-5}$  mol dm $^{-3}$ ) 23DNC solution containing  $\gamma$ -CD, respectively. The decrease in the fluorescence intensity of concentrated 23DNC solution is much remarkable than that of dilute 23DNC solution. When the  $\gamma$ -CD concentration is raised up to  $1.0 \times 10^{-2}$  mol dm $^{-3}$ , the 370-nm band at a low 23DNC concentration is sharpened compared to that at a high 23DNC concentration. This finding suggests that at least two kinds of inclusion complexes are present at a high concentration of 23DNC. Figure 16 shows the  $\gamma$ -CD concentration dependence of the fluorescence intensity, observed at 375 nm, for solutions of different 23DNC concentrations. At the same  $\gamma$ -CD concentration, the fluorescence intensity at a high 23DNC concentration is weak to a large extent, compared to the fluorescence intensity at a low 23DNC concentration. In dilute 23DNC solution, only a 1:1  $\gamma$ -CD–23DNC inclusion complex is most likely formed. Thus, we first estimated the  $K_1$  value of 23DNC for dilute 23DNC solution to be  $430 \pm 20$  mol $^{-1}$  dm $^3$ .

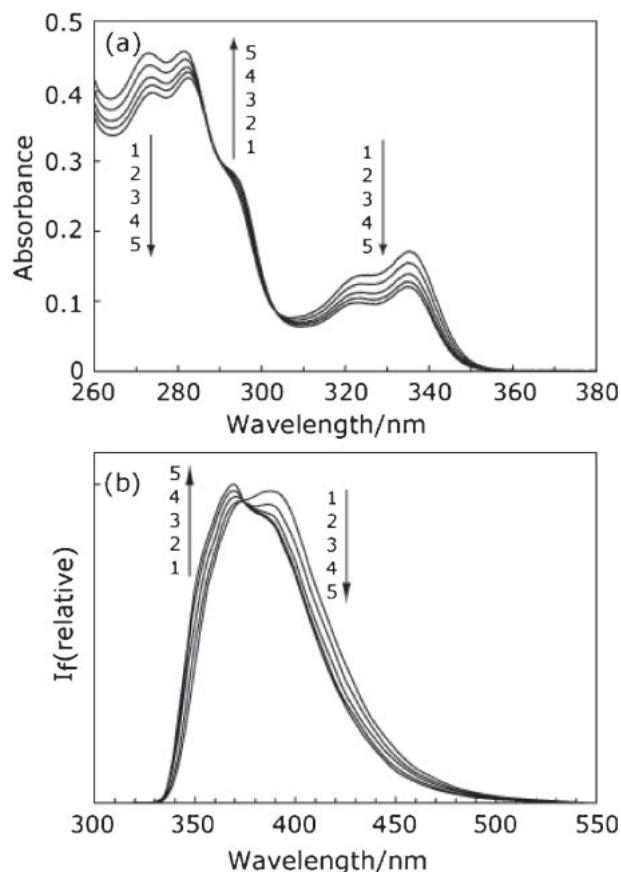


**Figure 14.** (a) Absorption spectra of 23DNC ( $9.7 \times 10^{-5} \text{ mol dm}^{-3}$ ) solution containing various concentrations of  $\beta$ -CD. Concentration of  $\beta$ -CD: (1) 0, (2)  $3.0 \times 10^{-4}$ , (3)  $1.0 \times 10^{-3}$ , (4)  $3.0 \times 10^{-3}$ , and (5)  $1.0 \times 10^{-2} \text{ mol dm}^{-3}$ . (b) Fluorescence spectra of 23DNC ( $4.8 \times 10^{-5} \text{ mol dm}^{-3}$ ) solution containing various concentrations of  $\beta$ -CD. Concentration of  $\beta$ -CD: (1) 0, (2)  $3.0 \times 10^{-4}$ , (3)  $1.0 \times 10^{-3}$ , (4)  $3.0 \times 10^{-3}$ , and (5)  $1.0 \times 10^{-2} \text{ mol dm}^{-3}$ .  $\lambda_{\text{ex}} = 305 \text{ nm}$ .

from the fluorescence intensity change. This  $K_1$  value of 23DNC is comparable with those ( $560 \pm 20$ ,  $310 \pm 60$ , and  $600 \pm 50 \text{ mol}^{-1} \text{ dm}^3$ ) of 2NC, 26DNC, and 27DNC (Table 2). Besides the 1:1  $\gamma$ -CD–23DNC inclusion complex, there may be a 1:2  $\gamma$ -CD–23DNC inclusion complex or a 2:2  $\gamma$ -CD–23DNC inclusion complex at high concentrations of 23DNC, although the excimer fluorescence is not observed in Figure 15a.

When the 1:2  $\gamma$ -CD–23DNC inclusion complex ( $\gamma\text{-CD} \cdot (23\text{DNC})_2$ ) is formed from the 1:1  $\gamma$ -CD–23DNC inclusion complexes ( $\gamma\text{-CD} \cdot 23\text{DNC}$ ), the fluorescence intensity of 23DNC is represented by

$$I_f = g[23\text{DNC}] + h[\gamma\text{-CD} \cdot 23\text{DNC}] + i[\gamma\text{-CD} \cdot (23\text{DNC})_2] \\ = (g + hK_1[\gamma\text{-CD}] + iK_1K_3'[\gamma\text{-CD}][23\text{DNC}])[23\text{DNC}] \quad (13)$$

Here,  $g$ ,  $h$ , and  $i$  are experimental constants including the fluorescence quantum yields of free 23DNC, the 1:1  $\gamma$ -CD–23DNC inclusion complex, and the 1:2  $\gamma$ -CD–23DNC inclusion complex, respectively. Under the assumption of a  $K_3'$  value, the concentration of free 23DNC can be calculated from the quadratic equation, which is similar to eq 10. Figure 16

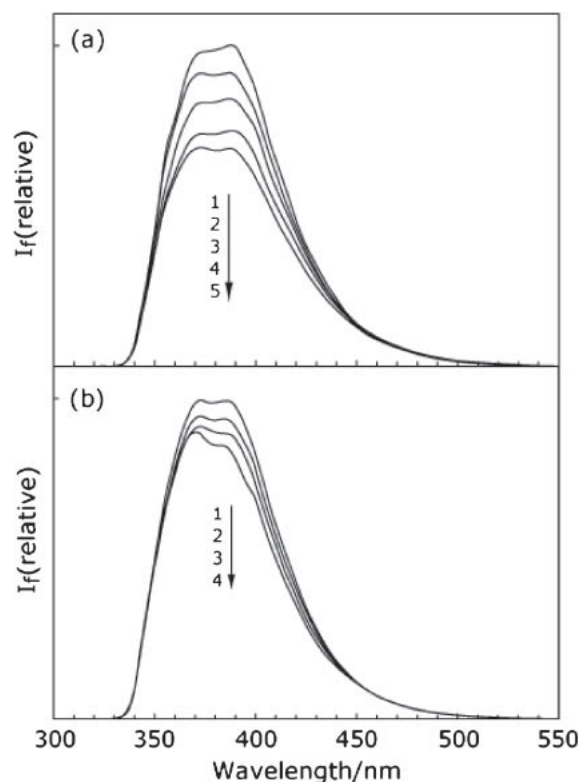


**Figure 15.** (a) Fluorescence spectra of concentrated 23DNC ( $9.7 \times 10^{-5} \text{ mol dm}^{-3}$ ) solution containing various concentrations of  $\gamma$ -CD. Concentration of  $\gamma$ -CD: (1) 0, (2)  $3.0 \times 10^{-4}$ , (3)  $1.0 \times 10^{-3}$ , (4)  $3.0 \times 10^{-3}$ , and (5)  $1.0 \times 10^{-2} \text{ mol dm}^{-3}$ .  $\lambda_{\text{ex}} = 309 \text{ nm}$ . (b) Fluorescence spectra of dilute 23DNC ( $1.1 \times 10^{-5} \text{ mol dm}^{-3}$ ) solution containing various concentrations of  $\gamma$ -CD. Concentration of  $\gamma$ -CD: (1) 0, (2)  $1.0 \times 10^{-3}$ , (3)  $3.0 \times 10^{-3}$ , and (4)  $1.0 \times 10^{-2} \text{ mol dm}^{-3}$ .  $\lambda_{\text{ex}} = 309 \text{ nm}$ .

exhibits best fit simulation curves, for which  $K_3'$  values at  $4.1 \times 10^{-5}$  and  $9.7 \times 10^{-5} \text{ mol dm}^{-3}$  of 23DNC are assumed to be  $2970$  and  $3190 \text{ mol}^{-1} \text{ dm}^3$ , respectively. The best fit simulation curves, which have been calculated on the basis of the scheme involving the formation of the 1:2 inclusion complex, well fit the observed fluorescence intensities observed at  $375 \text{ nm}$ . In addition, the  $K_3'$  values at different 23DNC concentrations are nearly the same, supporting the formation of the 1:2  $\gamma$ -CD–23DNC inclusion complex. To further confirm the formation of the 1:2 inclusion complex, similar simulations have been performed under the conditions that the fluorescence intensities, excited at different wavelengths, have been observed at  $390 \text{ nm}$ . The simulations for data excited at  $309$  and  $320 \text{ nm}$  gave  $K_3'$  values of  $2580$  and  $3180 \text{ mol}^{-1} \text{ dm}^3$ , respectively. These  $K_3'$  values are very close to that obtained at an observation wavelength of  $375 \text{ nm}$ , supporting that the 1:2  $\gamma$ -CD–23DNC inclusion complex truly exists.

If the 2:2  $\gamma$ -CD–23DNC inclusion complex ( $(\gamma\text{-CD})_2 \cdot (23\text{DNC})_2$ ) is formed, the fluorescence intensity is given as

$$I_f = g'[23\text{DNC}] + h'[\gamma\text{-CD} \cdot 23\text{DNC}] + i'[(\gamma\text{-CD})_2 \cdot (23\text{DNC})_2] \\ = (g' + h'K_1[\gamma\text{-CD}] + i'K_1^2K_3[\gamma\text{-CD}]^2[23\text{DNC}])[23\text{DNC}] \quad (14)$$

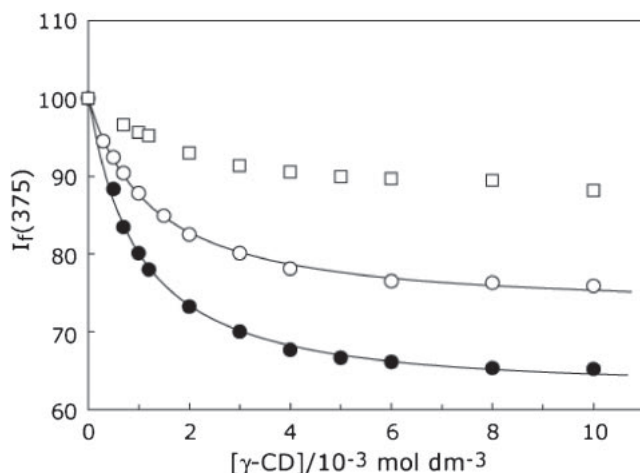


**Figure 16.** Simulation for the observed fluorescence intensities of 23DNC ( $\square$ :  $1.1 \times 10^{-5}$ ,  $\circ$ :  $4.1 \times 10^{-5}$ , and  $\bullet$ :  $9.7 \times 10^{-5} \text{ mol dm}^{-3}$ ) in aqueous solutions containing various concentrations of  $\gamma$ -CD. The fluorescence intensities in the absence of  $\gamma$ -CD have been normalized to 100. Best fit simulation curves, based on the scheme involving the 1:2  $\gamma$ -CD–23DNC inclusion complex, have been calculated with an evaluated  $K_1$  value of  $430 \text{ mol}^{-1} \text{ dm}^3$  and an assumed  $K_3'$  values of 2970 and  $3190 \text{ mol}^{-1} \text{ dm}^3$  at 23DNC concentrations of  $4.1 \times 10^{-5}$  and  $9.7 \times 10^{-5} \text{ mol dm}^{-3}$ , respectively.  $\lambda_{\text{ex}} = 309 \text{ nm}$ .  $\lambda_{\text{obs}} = 375 \text{ nm}$ .

where,  $g'$ ,  $h'$ , and  $i'$  are experimental constants including the fluorescence quantum yields of free 23DNC, the 1:1  $\gamma$ -CD–23DNC inclusion complex, and the 2:2  $\gamma$ -CD–23DNC inclusion complex, respectively. Assuming a  $K_3$  value, the concentration of free 23DNC can be calculated from the quadratic equation, which is similar to eq 8. Best fit simulation curves thus obtained fitted the observed fluorescence data, although the residual was slightly large, compared to the best fit simulation curves based on the scheme involving the 1:2  $\gamma$ -CD–23DNC inclusion complex. However, the  $K_3$  values at  $4.1 \times 10^{-5}$  and  $9.7 \times 10^{-5} \text{ mol dm}^{-3}$  of 23DNC were 26.4 and  $4.64 \times 10^4 \text{ mol}^{-1} \text{ dm}^3$ , respectively. The disagreement of the two  $K_3$  values at different 23DNC concentrations confirms no formation of the 2:2  $\gamma$ -CD–23DNC inclusion complex.

In the 1:1  $\gamma$ -CD–23DNC inclusion complex, two methoxycarbonyl groups are most likely extruded into the water environment. Consequently, the methoxycarbonyl groups extruded from the  $\gamma$ -CD cavity obstruct the association of the 1:1 inclusion complexes to form the 2:2  $\gamma$ -CD–23DNC inclusion complex. Within the 1:2  $\gamma$ -CD–23DNC inclusion complex, the steric hindrance of the methoxycarbonyl groups most likely prevents the overlapping of two naphthalene rings of 23DNC molecules, leading to no observation of the excimer fluorescence.

### Conclusion

$\beta$ -CD and TM- $\beta$ -CD form 1:1 inclusion complexes with 2NC, 27DNC, 26DNC, and 23DNC. For all the guests examined, the  $K_1$  value for  $\beta$ -CD is about five to ten times greater than that for TM- $\beta$ -CD. The inclusion mode of  $\alpha$ -CD depends on the shape of a guest molecule. 2NC, which has a

substituent at C<sub>2</sub> on a naphthalene ring, forms the 2:1  $\alpha$ -CD–2NC inclusion complex as well as the 1:1 inclusion complex. 26DNC, which has two substituents on C<sub>2</sub> and C<sub>6</sub> (substituents located on the line connecting C<sub>2</sub> and C<sub>6</sub>), forms the 2:1  $\alpha$ -CD–26DNC inclusion complex. On the other hand, 27DNC, in which a methoxycarbonyl group on C<sub>7</sub> is not located on the line connecting C<sub>2</sub> and C<sub>6</sub>, forms only the 1:1  $\alpha$ -CD–27DNC inclusion complex.  $\gamma$ -CD forms the 1:1 inclusion complex with 2NC. For long guest molecules (27DNC and 26DNC), 1:1 inclusion complexes associate to form the 2:2 inclusion complex. In the case of 23DNC, however, the 1:1  $\gamma$ -CD–23DNC inclusion complex associates with an additional 23DNC molecule to form the 1:2  $\gamma$ -CD–23DNC inclusion complex. In the  $\gamma$ -CD–23DNC inclusion complex, two substituents are likely extruded into the water environment from the  $\gamma$ -CD cavity. Due to the extruded substituents, two 1:1 inclusion complexes may not associate with to form a 2:2  $\gamma$ -CD–23DNC inclusion complex.

### Supporting Information

Absorption spectra of 27DNC in aqueous solutions containing  $\alpha$ - and  $\beta$ -CD, and double-reciprocal plots for 27DNC and 26DNC solutions containing  $\gamma$ -CD. This material is available free of charge on the web at <http://www.csj.jp/journals/bcsj/>.

### References

- W. Saenger, *Angew. Chem., Int. Ed. Engl.* **1980**, *19*, 344.
- M. L. Bender, M. Komiyama, *Cyclodextrin Chemistry*, Springer-Verlag, New York, **1978**.
- K. A. Connors, *Chem. Rev.* **1997**, *97*, 1325.
- R. J. Clarke, J. H. Coates, S. F. Lincoln, *Carbohydr. Res.* **1984**, *127*, 181.
- H. Hirai, N. Toshima, S. Uenoyama, *Bull. Chem. Soc. Jpn.* **1985**, *58*, 1156.
- R. J. Clarke, J. H. Coates, S. F. Lincoln, *J. Chem. Soc., Faraday Trans. 1* **1986**, *82*, 2333.
- S. Hamai, *Bull. Chem. Soc. Jpn.* **2000**, *73*, 861.
- C. Lee, Y. W. Sung, J. W. Park, *J. Phys. Chem. B* **1999**, *103*, 893.
- S. Hamai, *Bull. Chem. Soc. Jpn.* **2002**, *75*, 2371.
- K. Kano, I. Takenoshita, T. Ogawa, *Chem. Lett.* **1980**, 1035.
- D. M. Davies, M. E. Deary, *J. Chem. Soc., Perkin Trans. 2* **1996**, 2415.
- R. S. Murphy, T. C. Barros, J. Barnes, B. Mayer, G. Marconi, C. Bohne, *J. Phys. Chem. A* **1999**, *103*, 137.
- C. Retna Raj, R. Ramaraj, *J. Photochem. Photobiol., A* **1999**, *122*, 39.
- H.-R. Park, B. Mayer, P. Wolschann, G. Köhler, *J. Phys. Chem.* **1994**, *98*, 6158.
- a) S. Hamai, *J. Chem. Soc., Chem. Commun.* **1994**, 2243.  
b) S. Hamai, *J. Phys. Chem.* **1995**, *99*, 12109.
- E. K. Fraiji, Jr., T. R. Cregan, T. C. Werner, *Appl. Spectrosc.* **1994**, *48*, 79.
- a) G. Köhler, G. Grabner, C. Th. Klein, G. Marconi, B. Mayer, S. Monti, K. Rechthaler, K. Rotkiewicz, H. Viernstein, P. Wolschann, *J. Inclusion Phenom. Mol. Recognit. Chem.* **1996**, *25*, 103. b) G. Grabner, K. Rechthaler, B. Mayer, G. Köhler, K. Rotkiewicz, *J. Phys. Chem. A* **2000**, *104*, 1365.
- S. Hamai, *J. Phys. Chem. B* **1997**, *101*, 1707.

- 19 S. Hamai, *J. Inclusion Phenom. Mol. Recognit. Chem.* **1997**, 27, 57.
- 20 H. Dodziuk, J. Sitkowski, L. Stefaniak, D. Sybilska, J. Jurczak, *Supramol. Chem.* **1996**, 7, 33.
- 21 A. Granados, R. H. de Rossi, *J. Am. Chem. Soc.* **1995**, 117, 3690.
- 22 N. Funasaki, Y. Uemura, S. Hada, S. Neya, *J. Phys. Chem.* **1996**, 100, 16298.
- 23 R. L. Schiller, S. F. Lincoln, J. H. Coates, *J. Chem. Soc., Faraday Trans. 1* **1987**, 83, 3237.
- 24 C. R. Raj, R. Ramaraj, *Chem. Phys. Lett.* **1997**, 273, 285.
- 25 S. Hamai, *Bull. Chem. Soc. Jpn.* **2008**, 81, 574.
- 26 a) S. Hamai, *Bull. Chem. Soc. Jpn.* **1982**, 55, 2721. b) S. Hamai, *Bull. Chem. Soc. Jpn.* **1996**, 69, 543. c) S. Hamai, N. Mononobe, *J. Photochem. Photobiol., A* **1995**, 91, 217.
- 27 T. Tamaki, T. Kokubu, K. Ichimura, *Tetrahedron* **1987**, 43, 1485.
- 28 T. C. Barros, K. Stefaniak, J. F. Holzwarth, C. Bohne, *J. Phys. Chem. A* **1998**, 102, 5639.
- 29 J. M. Madrid, F. Mendicuti, *Appl. Spectrosc.* **1997**, 51, 1621.
- 30 J. M. Madrid, J. Pozuelo, F. Mendicuti, W. L. Mattice, *J. Colloid Interface Sci.* **1997**, 193, 112.
- 31 J. M. Madrid, F. Mendicuti, W. L. Mattice, *J. Phys. Chem. B* **1998**, 102, 2037.
- 32 C. Alvariza, R. Usero, F. Mendicuti, *Spectrochim. Acta, Part A* **2007**, 67, 420.
- 33 M. Cervero, F. Mendicuti, *J. Phys. Chem. B* **2000**, 104, 1572.
- 34 A. D. Marino, F. Mendicuti, *Appl. Spectrosc.* **2002**, 56, 1579.
- 35 S. Hamai, A. Nakamura, in *Handbook of Photochemistry and Photobiology, Volume 3: Supramolecular Photochemistry*, ed. by H. S. Nalwa, American Scientific Publishers, Stevenson Ranch, **2003**, pp. 59–119.
- 36 a) J. A. Hamilton, *Carbohydr. Res.* **1985**, 142, 21. b) S. Hamai, *J. Phys. Chem.* **1989**, 93, 6527. c) S. Makedonopoulou, M. Mavridis, *Acta Crystallogr., Sect. B* **2000**, 56, 322.